Hindawi
Adsorption Science & Technology
Volume 2022, Article ID 4143138, 13 pages
https://doi.org/10.1155/2022/4143138

Research Article

An Effective Biomass for the Adsorption of Methylene Blue Dye and Treatment of River Water

Shaziya H. Siddiqui,[1] **Mohammad Kashif Uddin**,[2] **Runit Isaac**,[1] **and Obaid F. Aldosari**[2]

[1]*Department of Chemistry, Sam Higginbottom University of Agriculture Technology & Sciences, Allahabad 211007, India*
[2]*Department of Chemistry, College of Science, Majmaah University, Al-Majmaah, 11952, Saudi Arabia*

Correspondence should be addressed to Shaziya H. Siddiqui; shaziya.shoaib@gmail.com, Mohammad Kashif Uddin; mohdkashifchem@gmail.com, and Obaid F. Aldosari; o.aldosari@mu.edu.sa

Received 16 June 2022; Revised 31 July 2022; Accepted 4 August 2022; Published 29 September 2022

Academic Editor: Qiao Chen

Neolamarckia cadamba leaves were used as an adsorbent for methylene blue removal as well as for the reduction in the water quality parameters of the sewage belts of Yamuna River in Allahabad, Uttar Pradesh, India. A variety of water quality parameters were assessed, including chemical oxygen demand, biological oxygen demand, total dissolved solids, conductivity, hardness, pH, and temperature. A great deal of degradation in the water quality parameters collected from three locations within the Yamuna River in Allahabad, Uttar Pradesh, India, has been observed by treating with *Neolamarckia cadamba* leaves. The adsorption studies were carried out by the batch method, and the effect of various parameters such as contact time, pH, initial concentration, and temperature was assessed. The maximum removal of methylene blue was obtained at pH 5 after 120 minutes of equilibrium time. In addition to fitting the Langmuir isotherm most accurately, the adsorbent also followed pseudokinetics of the second order. The maximum monolayer adsorption capacity of used biomass was 101 mg/g using 50 mg/L methylene blue solution. It is evident from the thermodynamic data that the adsorption is exothermic. Also, the spontaneity of the interaction between adsorbent and adsorbate decreases with temperature. Energy-dispersive X-ray spectroscopy, scanning electron microscopy, and Fourier transform infrared spectroscopy techniques were used to characterize the adsorbent. SEM images revealed that the biomass consisted of irregular spherical lumps with a porous structure, which provided effective adsorption sites. A chemical composition analysis of the biomass by EDAX shows that the chemical composition of oxygen and carbon decreases, whereas nitrogen's chemical composition increases.

1. Introduction

The existence of living organisms on today's planet is greatly affected by water pollution. The sewage discharge from industries contains various organic and inorganic pollutants that are directly discharged into lakes and rivers affecting the flora and fauna of the ecosystem. The water standards like biological oxygen demand (BOD), chemical oxygen demand (COD), pH, total dissolved solids (TDS), conductivity, and hardness level of the river water should be maintained according to the standards provided by the environmental pollution agency (EPA) and World Health Organization (WHO). There have been some recent studies reporting on the quality of river water [1, 2], There are many toxic pollutants such as heavy metals, dyes, phenols, nitrobenzene, and pesticides released by various industries such as battery manufacturing, paint industries, textile manufacturing, pharmaceutical, and electroplating manufacturing. Synthetic dyes are toxic to human beings and aquatic organisms. The biodegradation of synthetic dyes is not easily possible because the microorganism cannot damage the aromatic ring of synthetic colorants [3]. Methylene blue (MB) dye is a cationic dye and is also known as tetraethylthionine hydrochloride. MB is a hazardous textile dye that is used in the dyeing of silk, leather, paper, and ink preparation. This dye show toxicity such as mutagenicity, neurotoxicity, and nucleic acid damage causing various health problems such as high pulse rate, jaundice, tissue necrosis, cyanosis, and limb paralysis [4]. When released into the environment, MB is a hazardous synthetic dye with a complex aromatic molecular structure [5].

There have been many physiochemical methods studied to treat dye-containing wastewater, but adsorption is the most appropriate because it is economical, feasible, and can work at high dye concentrations. Many agricultural wastes have been used for the adsorption of toxic aqueous pollutants such as walnut shell [5], Punica granatum [6], leechi peel [7], Schleichera oleosa bark [8], rice husk derivatives [9], Onosma bracteatum [10], Coriandrum sativum [11], and most recently, rubber seed pericarp [12]. For the adsorption of toxic pollutants, other synthesized adsorbents such as MOF-5/Cu [13], CuCl-MIL-47 [14], mesoporous silica/DZ [15], and magnetic mesoporous silica [16] have also been used. According to literature on the removal of MB using natural materials, biomass is an effective adsorbent for the removal of MB. A study by Ramutshatsha et al. showed that 98% of the MB was removed with waste orange and lemon peels [17]. In a study by Omorogie et al., Nauclea diderrichii activated carbon-agricultural waste was used to remove MB, and an adsorption capacity of 35.09 mg/g was determined [18].

Neolamarckia cadamba (NC) or Kadam also known as burflower belongs to the family *Rubiaceae*. The plant contains anti-inflammatory, antidiabetic, and antipyretic effects. Leaf decoction is used to treat aphthae or stomatitis, ulcers, and wounds. NC leaf extract has a hypoglycemic effect. Chemical elements such as indole alkaloids, terpenoids, saponins, sapogenins, terpenes, steroids, lipids, reducing sugar, glycosides, and flavonoids were found in different parts of NC during phytochemical analysis. The glycosidic indole alkaloids cadambine, 3alpha-dihydrocadambine, and isodihydrocadambine and two related nonglycosidic alkaloids are the isolated principles. In this study, NC as an adsorbent was found effective in methylene blue dye removal due to its porous structure. The adsorbent also shows effective results in the reduction of water quality of Yamuna River which is located on the bank of Allahabad, Uttar Pradesh, India.

For samples collected from the three sewage belts of Chachar, Katghar, and Kareli near the outskirts of the Yamuna River in an interval of months and from point stream, upstream, and downstream, BOD, COD, pH, temperature, TDS, conductivity, and hardness were monitored. The water samples were then treated with NC as an adsorbent, and the change in the water sample parameters after adsorption was reported. Simultaneously, batch adsorption of MB was carried out using NC leaves. The kinetics, isotherm, and thermodynamic studies were explored.

2. Materials and Methods

2.1. Instrument and Chemicals. The solutions of manganese sulfate, sodium azide, ferrous ammonium sulfate, concentrated H_2SO_4, sodium thiosulfate, ferroin indicator, starch indicator, potassium dichromate, mercuric sulfate, methylene blue, and silver sulfate were prepared using double distilled water. All the chemicals purchased were of analytical grade. A scanning electron microscope was used to study surface characteristics (SEM, Zeiss, CIL, BHU, India), Fourier transform infrared spectroscopy was used to study functional groups (Perkin Elmer, USA, model spectrum-BX, range 4,000-400 cm^{-1}), and X-ray energy-dispersive spectroscopy was used to determine element presence (EDAX, Zeiss, CIL, BHU, India). The BOD incubator (impact instruments, India) was used for the BOD study, and the COD open reflux digester (impact instruments, India) was used for the COD measurement. A pH meter, TDS meter, and conductivity meter made by Labtronics instruments, India, were used to measure water quality parameters. The adsorption analysis was carried out by using a UV-visible spectrophotometer (Globe instruments) at 664 nm.

2.2. Preparation of Adsorbent. The collection of the adsorbent was through the local area of the SHUATS university campus, Allahabad, India. NC leaves were collected and washed in distilled water for the removal of existing impurities. NC leaves were then ground to a fine powder and sieved to 120-180 microns in size. The prepared biomass was used as such for adsorption studies.

2.3. Water Sampling. A total of 48 wastewater samples were collected from the mainstream, downstream, and upstream areas of the Yamuna River in Allahabad, Uttar Pradesh, India, including Katghar, Chachar, and Kareli sewage belts. The two-month samples (February and March) were collected and analyzed. The parameters like BOD, COD, pH, TDS, conductivity, and hardness were studied according to the procedure mentioned in the American Public Health Association (APHA) manual. Remediation of parameters for the water quality assessment was performed using NC leaves. 0.1 g of NC leaves was used to treat wastewater samples collected from three locations at both sampling areas.

2.4. Batch Adsorption Study. Experimental studies of MB adsorption by using NC leaves were performed under batch conditions. The experiments were carried out in a 100 mL conical flask containing 25 mL of 50 mg/L MB solution equilibrated with 0.1 g adsorbent for 24 hrs. The experiments were performed for different initial dye concentrations (10-100 mg/L) to find the effect of the concentration of MB adsorption. The solution was filtered, and the supernatant obtained was made to be analyzed by a UV-visible spectrophotometer with a maximum absorbance of 664 nm. The pH was measured between 2 and 8 and adjusted by dropwise addition of 0.5 M HCl and NaOH. All experiments were performed in triplets. The following formulas were used to compute the capacity of adsorption (q_e) and percentage of removal (% removal):

$$\%\text{removal} = \frac{(C_0 - C_e) \times 100}{C_0}, \qquad q_e = \frac{(C_0 - C_e) \times V}{W}, \tag{1}$$

where C_o is the initial concentration of the adsorbate (mg/L), C_e is the equilibrium concentration of the adsorbate (mg/L), q_e is the adsorption capacity at equilibrium (mg/L), V is the volume of the solution in L, and W is the weight of the adsorbent in g.

2.5. Error Analysis. The excel function and origin Pro21 software were used to evaluate the models using various error functions. The various error functions are given in the following equations:

$$\begin{aligned}
\text{RMSE} &= \sqrt{\frac{1}{N-2}\sum_{i=1}^{n}\left(q_{e\text{model}} - q_{e\text{cal}}\right)},\\
\text{ARE} &= \frac{100}{P}\sum_{i=0}^{n}\frac{\left(q_{e\text{model}} - q_{e\text{cal}}\right)}{q_{e\text{model}}},\\
\text{Hybrid} &= \frac{100}{N-P}\sum_{i=1}^{n}\frac{\left(q_{e\text{model}} - q_{e\text{cal}}\right)^2}{q_{e\text{cal}}},\\
\text{MPSD} &= 100\times\sqrt{\frac{1}{N-P}\sum_{i=1}^{n}\frac{\left(q_{e\text{model}} - q_{e\text{cal}}\right)^2}{q_{e\text{cal}}}},\\
x^2 &= \sum_{i=1}^{n}\frac{\left(q_{e\text{model}} - q_{e\text{cal}}\right)^2}{q_{e\text{cal}}}.
\end{aligned} \tag{2}$$

3. Results and Discussion

3.1. Characterization. The high porosity of the adsorbent can be determined by the SEM images. A micrograph of NC leaf materials shows impurities and fragments, which appear as bars or wires (Figure 1(a)). This phenomenon was also reported by Peng et al. [19] and Yu et al. [20]. Following MB loading, the surface morphology of NC leaves was more regular than the unloaded sample (Figure 1(b)). Besides, the SEM images revealed that the biomass consisted of irregular spherical lumps with a porous structure, which provided effective adsorption sites for MB and thus occupy the pores after successful adsorption. The dye solution occupies the pores after adsorption as shown in Figures 1(a) and 1(b). The EDAX data show the elemental composition of unloaded and MB loaded NC leaves (Figures 2(a) and 2(b)). The EDAX analysis reveals that the elements present before and after adsorption are carbon, nitrogen, oxygen, calcium, and potassium, as observed in Figures 2(a) and 2(b). It was found that the amount of carbon and oxygen reduced after MB adsorption. The chemical composition (%) of carbon was 61.21% before adsorption which slightly reduced to 60.46% after adsorption while the chemical composition (%) of oxygen composition decreased from 37.42% to 18.64% after adsorption. A sharp increase in nitrogen chemical composition (%) from 1.48 to 19.76% indicates that MB has been successfully absorbable on the material's surface.

The FTIR analysis of NC biomass on loaded MB and unloaded NC leaves is shown in Figure 3. The peak at 3383.39 cm^{-1} and 3356.50 cm^{-1} indicates the presence of free –OH groups [21]. The peak near 2920 cm^{-1} ascertain to -CH stretching. The peaks near 1623 and 1735 cm^{-1} correspond to $-NH_2$ deformation and the –C=O group, respectively [22]. The peaks at 1460 cm^{-1} and 1160 cm^{-1} correspond to C-CH_3 deformation and C-N stretching. The common admixtures such as quartz with characteristic absorption bands at 642–646 cm^{-1}, 782 cm^{-1}, and 797–801 cm^{-1} and amorphous silica at 892.85 cm^{-1} are also clearly indicative [23].

3.2. Water Sampling Parameters. During February and March 2019, a monthly water sampling was performed. The samples were collected from three locations, i.e., Katghar, Chachar, and Kareli sewage belts of Yamuna River, Allahabad, and satellite locations are shown in Figures 4(a) and 4(b). The water samples were collected from the point source and 50 m upstream and downstream. The analysis of wastewater samples from different locations after treatment with the adsorbent (NC leaves) is reported in Tables 1 and 2, and the % decrease in water quality parameters can be seen in Table 3 and is shown in Figure 5. According to WHO, the WHO permissible limit of pH for marine organisms is around 6.5-9.0 and for drinking and irrigation purposes is 6.5 to 8.4 (WHO, 2008). Based on the results, all sewage belts have pH levels of around 9-10, which shows that the water is alkaline and not harmful, but not recommended for drinking. For sampling area 1, TDS levels are in the range of 304-350 mg/L, which indicates good water quality as they fall within the permissible limit for drinking. According to the data, as the temperature increases, the TDS level also increases in the range of 450-460 mg/L, which is above 300 mg/L, showing deposition of dissolved salts from agricultural and industrial drains. Due to the correlation between conductivity and TDS, the TDS level increases with an increase in water temperature.

The degree of hardness is a popular way to classify hardness as soft water in the range of 75 mg/L, moderate water as 75 mg/L to 150 mg/L, hard water in the range of 150-300 mg/L, and very hard water above 300 mg/L according to BIS, WHO. The water samples for all three locations show that water is hard as hardness lies in the range of 150-300 mg/L due to the presence of calcium and magnesium salts of carbonates, bicarbonates, sulfates, and chlorides [1, 2]. The BOD values for sample locations in sampling areas are in the gamut of 1-20 mg/L within the permissible limit of CPCB (central pollution control board) which is less than 30 mg/L. In the sampling areas, COD values within the range of 20-300 mg/L were within the permissible range of 250 mg/L for CPCB. In one sample, COD exceeded the permissible limit, perhaps due to dissolved organics. According to Table 1, the BOD/COD ratio serves as an indicator of river pollution; it reflects organic pollutants' biodegradability. For Katghar and Chachar, the BOD/COD ratios are around 0.2, indicating biodegradability, while for Kareli stream, the ratio is below 0.05, indicating toxicity.

The wastewater samples collected from three belts of Yamuna River were treated with NC leaves. The results are reported in Table 3 and Figure 5. The results show a decrease in water quality parameters like COD, hardness, TDS, and electrical conductivity after treatment with the adsorbent. The decrease in concentration levels of all four cases was reported after treatment with adsorbent. The absorbent

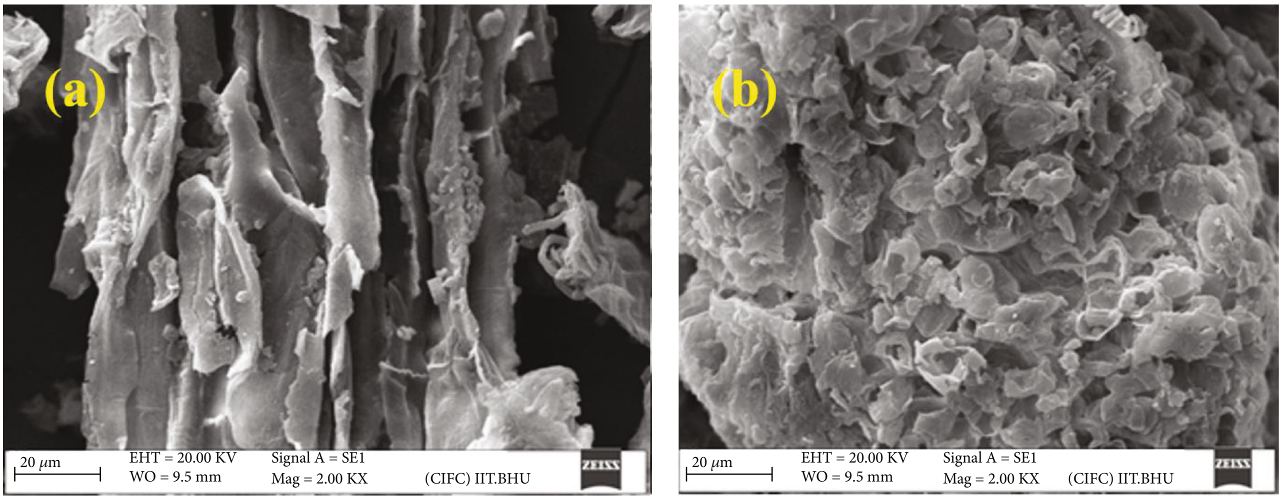

(a) (b)

FIGURE 1: SEM image of *Neolamarckia cadamba*: (a) unloaded; (b) loaded with methylene blue.

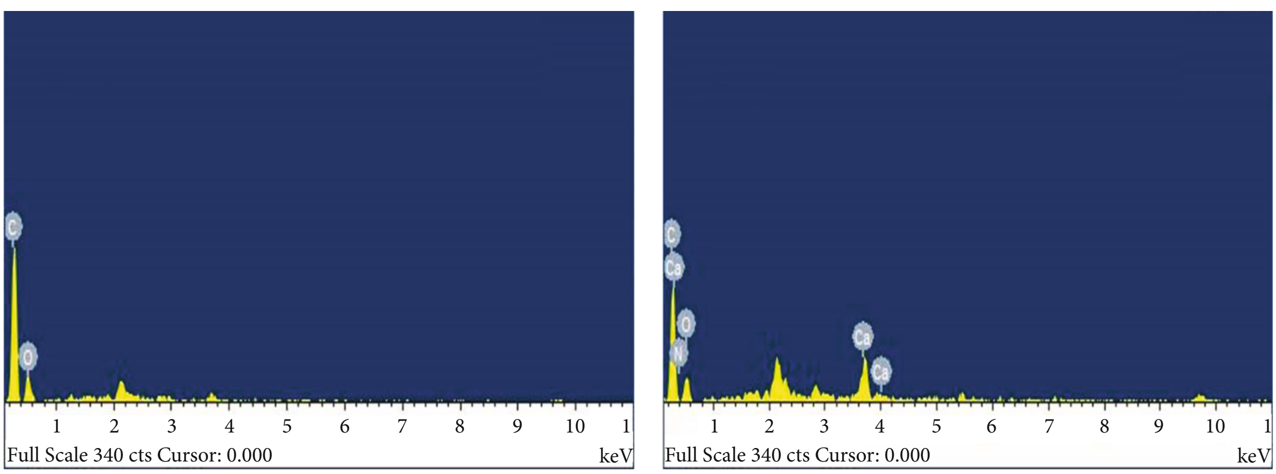

(a) (b)

FIGURE 2: EDAX analysis of *Neolamarckia cadamba*: (a) unloaded; (b) loaded with methylene blue.

shows a good decrease in the values of TDS and hardness for all the sampling locations. This is due to the high adsorption capacity of NC leaves and porosity [24]. Hence, the adsorbent can be used for the treatment of the quality of the river water due to its good absorptive property.

3.3. Contact Time and Kinetic Study. The effect of contact time on MB adsorption was measured in the range of 5 to 180 minutes and at 30°C. The adsorption was rapid at first, but soon slowed. Initially, the adsorption was fast in the beginning due to the sorption of dyes on the unfilled area, and a slowdown in adsorption occurred later when the sites were occupied. In 120 minutes, the equilibrium was reached, and after that, the adsorption of MB declined as shown in Figure 6(a). It is because dye molecules tend to aggregate, making them difficult to adsorb. The same result was noted by El-sayed, for the adsorption of MB onto palm kernel fiber [25].

To predict the kinetics of MB onto NC leaves, various kinetic models were used such as pseudo-first-order, pseudo-second-order, intraparticle diffusion, and Elovich equation.

A linear pseudo-first-order equation is given as

$$\log (q_e - q_t) = \log q_e - \frac{k_1 t}{2.303}, \quad (3)$$

where q_e is adsorption capacity at equilibrium for dye solution (mg g^{-1}) and q_t (mg g^{-1}) is dye solution's adsorption capacity at time t for k_1 is the rate constant (min^{-1}). The result of log (q_e-q_t) vs. t plot is reported in Table 4. As the experimental q_e value does not match the calculated q_e value, and the R^2 value is also low, the MB adsorption cannot follow pseudo-first-order kinetics.

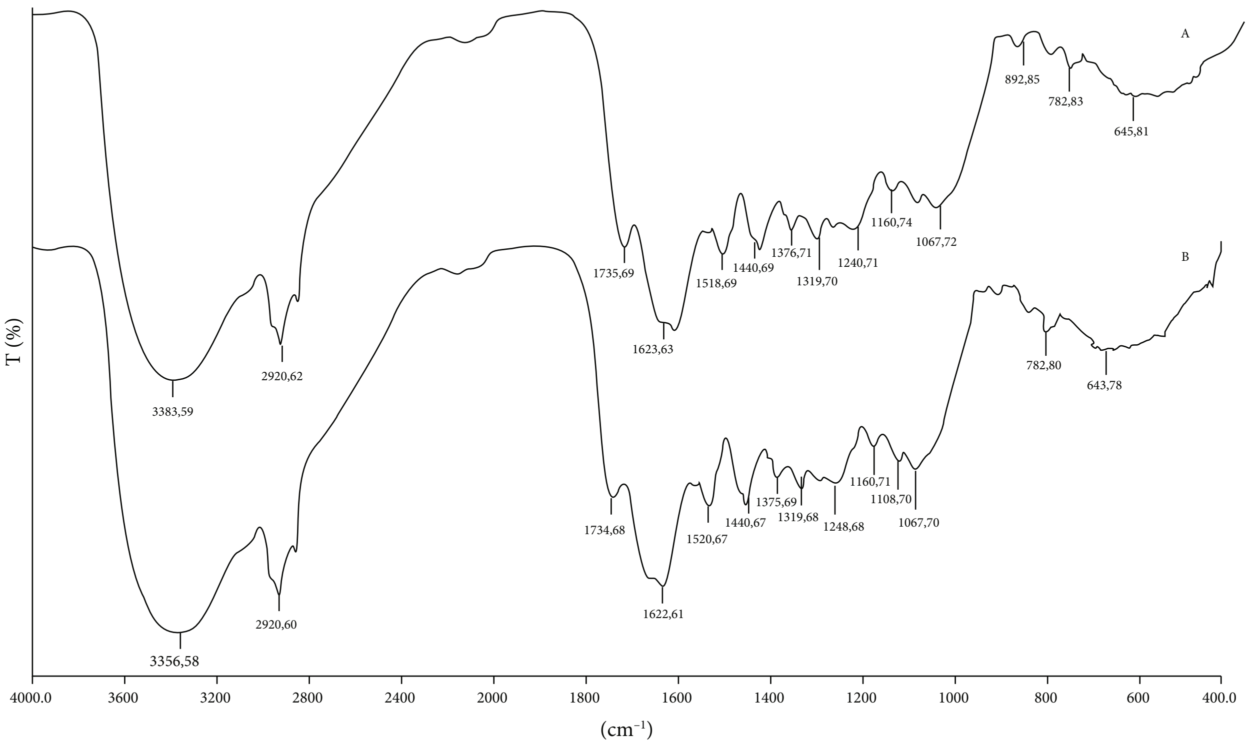

Figure 3: FTIR spectra of (a) unloaded *Neolamarckia cadamba*; (b) loaded with methylene blue of *Neolamarckia cadamba* leaves.

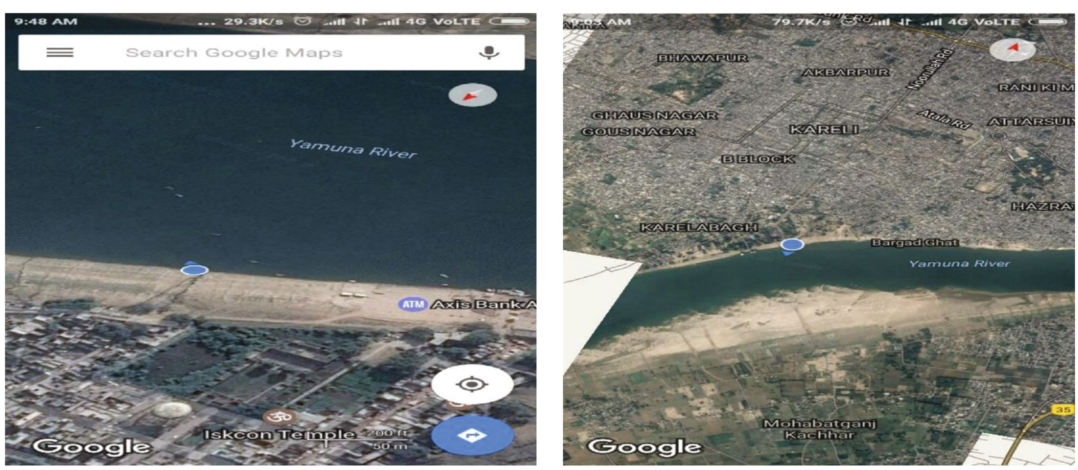

(a) (b)

Figure 4: (a, b) Location of water sampling.

The linear pseudo-second-order equation is given as

$$\frac{t}{q_t} = \frac{1}{k_2} q_e{}^2 + \frac{t}{q_e}. \quad (4)$$

q_e is the adsorption capacity of dye solution at equilibrium (mg/g), q_t is the adsorption capacity at time t for dye solution (mg/g), and k_2 is the constant for 2nd order (g/mg/min). A plot of t/q_t vs. t was plotted as shown in Figure 6(b) and reported in Table 4. According to the data, the q_e experimental value matches the q_e calculated value, and the R^2 value is also higher, so the adsorption of MB onto NC was followed by pseudo-second-order kinetics.

The adsorption process can also be determined using the diffusion model based on pore diffusion. The intraparticle diffusion model is given as

$$q_t = K_{\mathrm{id}} t^{1/2} + C, \quad (5)$$

where q_t is the adsorption capacity of dye solution at time t (mg/g) and K_{id} is the intraparticle diffusion constant. The values of K_{id}, C, and R^2 values are calculated from the plot

Table 1: First water sampling parameter analysis done on 02.02.19 for three locations of Yamuna River.

Sampling area	pH	Temperature (°C)	TDS (mg/L)	Conductivity (mΩ cm^{-1})	BOD (mg/L)	COD (mg/L)	BOD/COD	Hardness (mg/L)
Katghar								
Upstream (50 m)	9.7	18.9	304	0.996	6.03	340	0.017	200
Point stream	9.8	19	332	0.976	16.2	144	0.112	250
Downstream (50 m)	9.6	19.1	322	0.976	9.73	20	0.486	200
Chachar								
Upstream (50 m)	9.7	19.3	316	0.962	4.8	40	0.12	169
Point stream	9.6	19.2	319	0.988	6.4	36	0.177	170
Downstream (50 m)	9.7	19.3	348	0.988	3.6	32	0.112	169
Kareli								
Upstream (50 m)	9.7	19.9	320	1.054	2.46	80	0.03	200
Point stream	10	19.6	332	1.038	5.06	60	0.084	240
Downstream (50 m)	9.6	21	358	1.08	1.71	20	0.085	150

Table 2: Second sampling done on 06.03.19 for three locations of Yamuna River.

Sampling area	pH	Temperature (°C)	TDS (mg/L)	Conductivity ($m\Omega\ cm^{-1}$)	BOD (mg/L)	COD (mg/L)	BOD/COD	Hardness (mg/L)
Katghar								
Upstream (50 m)	9.5	24.2	456	1.36	1.93	60	0.032	200
Point stream	9.6	25	463	1.356	3.3	120	0.027	225
Downstream (50 m)	9.6	23.8	455	1.314	2.4	90	0.026	200
Chachar								
Upstream (50 m)	9.5	23.4	450	1.32	3.2	148	0.021	210
Point stream	9.6	23.5	455	1.324	6.73	124	0.054	160
Downstream (50 m)	9.6	23.4	446	1.29	5.1	112	0.045	230
Kareli								
Upstream (50 m)	9.6	24.2	456	1.3	1.4	45	0.031	200
Point stream	9.5	25	463	1.304	3.6	122	0.029	230
Downstream (50 m)	9.6	23.8	455	1.3	1.26	30	0.042	200

Table 3: Adsorption effect of *Neolamarckia cadamba* leaves on water quality parameters of three locations of Yamuna River.

Parameters	Before adsorption			After adsorption					
1st sampling	Katghar	Chachar	Kareli	Katghar	% decrease	Chachar	% decrease	Kareli	% decrease
TDS (mg/L)	332	319	332	264	20.48	289	9.40	242	27.10
Conductivity	0.976	0.988	1.038	0.762	21.9	0.862	12.75	0.838	19.26
Hardness (mg/L)	250	200	200	35	86	25	87.5	25	87.5
COD (mg/L)	144	36	60	50	65.2	15	58.3	20	66.6
2nd sampling	Katghar	Chachar	Kareli	Katghar	% decrease	Chachar	% decrease	Kareli	% decrease
TDS (mg/L)	463	455	463	397	14.25	382	16.04	397	8.65
Conductivity	1.356	1.324	1.304	1.192	12.09	1.15	13.11	1.20	7.97
Hardness (mg/L)	225	160	230	30	86.6	25	84.3	25	89.1
COD (mg/L)	120	124	122	80	33.3	60	51.6	65	46.7

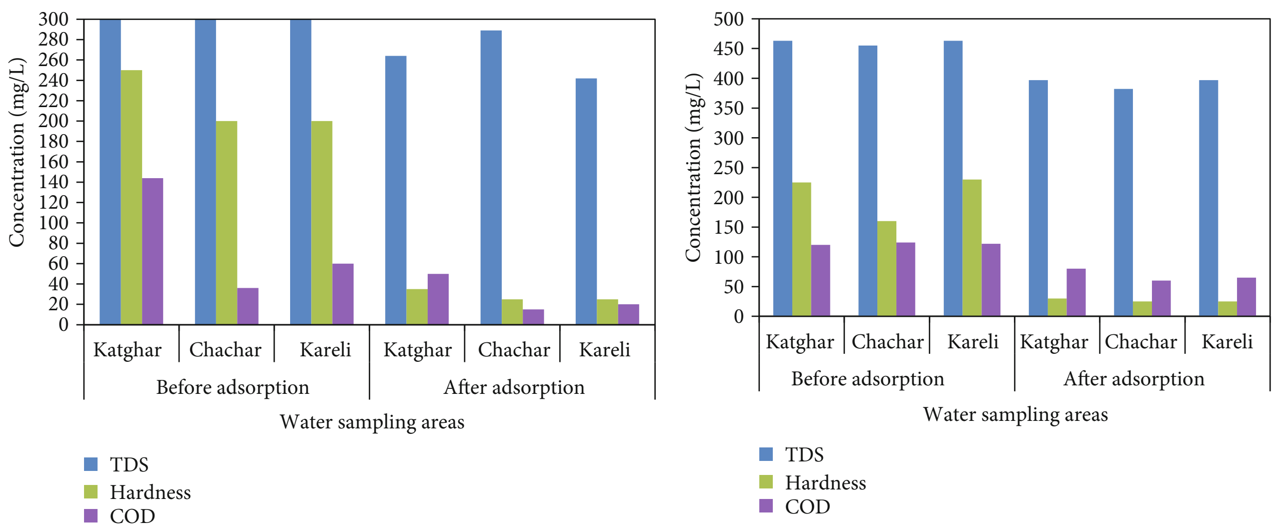

(a)

(b)

Figure 5: Graphical representation of the analysis conducted for various water quality parameters at different locations collected at (a) sampling area 1; (b) sampling area 2.

of q_t vs. $t^{1/2}$ and reported in Table 4. It is found that the intraparticle diffusion model is the only rate-determining step. The intercept value is indicative of the boundary-layer thickness. The thickness of the border layer can be directly correlated with the intercept value [4].

The Elovich equation:

$$q_t = A + B \ln T. \quad (6)$$

A and *B* are Elovich constants. The Elovich equation is used to describe the process of chemisorptions.

3.4. Effect of pH. Among numerous parameters for the adsorption of pollutants by utilization of waste materials, pH is the most critical. It was decided to study the adsorption process at pH 5 because from the results it was observed that the amount of MB adsorbed increases from 2 to 5 values of pH but decreases after pH value 5 (Figure 7). Due to a lower pH (<2), H^+ ion in the solution will further disrupt the bonding between the adsorbent and the MB dye, since more carboxyl and siloxane groups in the adsorbent will bind the H^+ and become positively charged. At higher pHs, the dye was unable to capture OH^- in the solution, so there was free OH^- in the solution. The carboxyl group in the adsorbent was a partially positive active group, which means that when the color base is added, it tends to be partially negative in nature. As a result, dye and free OH^- ion competed for the surface of the adsorbent, resulting in a decrease in dye adsorption. The solution pH changes with the interaction between MB and NC leaves during the adsorption process since the charges are dependent on the pH in the aqueous phase.

3.5. Adsorption Isotherm. To observe the adsorption behavior of NC leaves onto MB, there are a variety of isotherm models such as Langmuir, Freundlich, Temkin, and D-R.

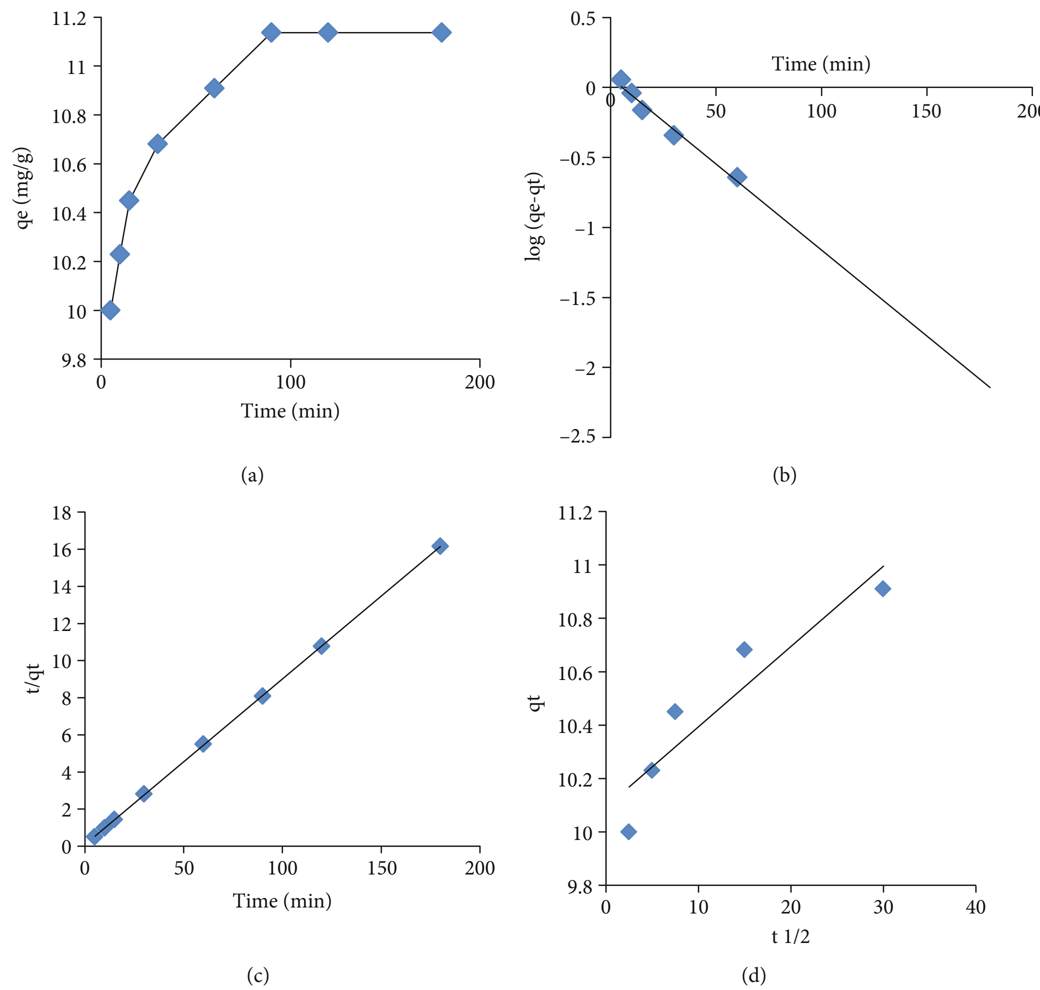

Figure 6: (a) Effect of contact time; (b) pseudo-first-order kinetics; (c) pseudo-second-order kinetics; (d) intraparticle diffusion model for the adsorption of methylene blue onto *Neolamarckia cadamba*.

Table 4: Kinetic parameters for the removal of methylene blue on *Neolamarckia cadamba* leaves.

Kinetic model	Parameters	Values
Pseudo-first-order	$q_{e(cal)}$ (mg g^{-})	1.169
	$q_{e(exp)}$ (mg g^{-1})	11.167
	k_1 (min^{-1})	0.0283
	R^2	0.9765
Pseudo-second-order	$q_{e(cal)}$ (mg g^{-})	11.21
	$q_{e(exp)}$ (mg g^{-1})	11.167
	k_2 (g mg^{-1} min^{-1})	1
	R^2	0.0859
Intraparticle diffusion model	K_{id}	0.03
	C	10.094
	R^2	0.8605
Elovich model	A	9.48
	B	0.3414
	R^2	0.9748

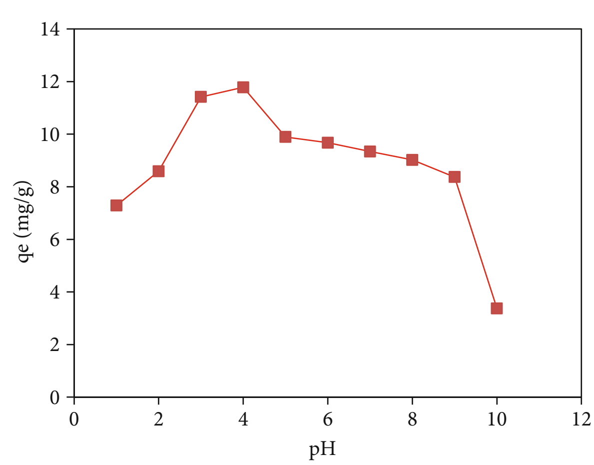

Figure 7: Effect of pH for the adsorption of MB ions onto *Neolamarckia cadamba* leaves.

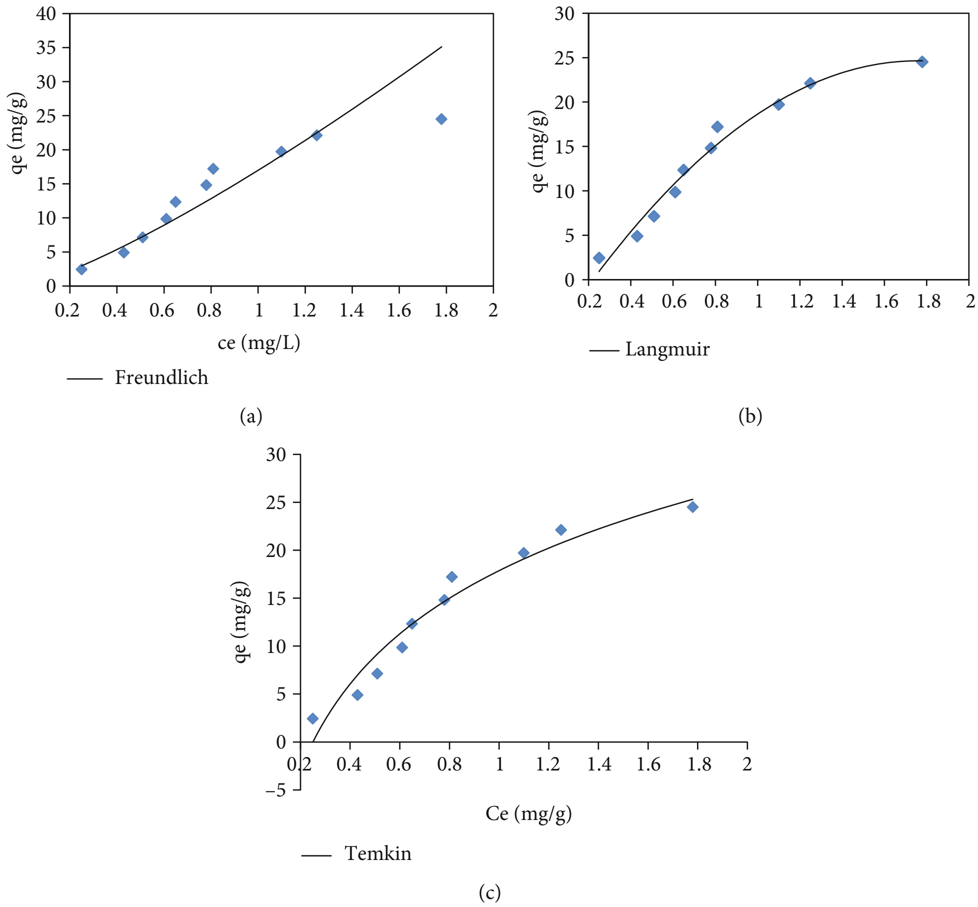

FIGURE 8: (a) Freundlich isotherm plot; (b) Langmuir isotherm plot for the adsorption of methylene blue onto *Neolamarckia cadamba* leaves; (c) Temkin isotherm plot for the adsorption of methylene blue onto *Neolamarckia cadamba* leaves.

The Langmuir model suggests that dynamic monolayer formation, i.e., molecules absorb and are desorbed under the same equilibrium conditions, occurred on the homogenous surfaces (all binding sites having the same energy). The nonlinear equation of Langmuir isotherm is given as

$$q_e = \frac{q_{\max} b C_e}{1 + bC_e}, \quad (7)$$

where q_e is the equilibrium adsorption capacity at various concentrations (mg/g), q_m is dye solution monolayer adsorption capacity (mg/g), C_e is the adsorbate concentration (mg/L), and b is the Langmuir constant (L/mg). A plot of $1/q_e$ vs. $1/C_e$ is plotted as shown in Figure 8(b), and values are given in Table 5.

The Freundlich isotherm model considers surface heterogeneity and multilayer adsorption. The nonlinear form of its equation is given as

$$q_e = K_F C_e^{1/n}, \quad (8)$$

where q_e is the adsorption capacity at equilibrium (mg/g) and n and K_f are Freundlich constants. A plot of log q_e vs.

TABLE 5: Adsorption isotherm for the removal of methylene blue on *Neolamarckia cadamba* leaves.

Isotherm	Parameters	Values
Langmuir	$q_{\max}$	101.4
	b	0.2001
	R^2	0.903
	Chi-sqr	5.37
Freundlich	n	1.14
	K_f	16.57
	R^2	0.8862
	Chi-sqr	6.33
Temkin	B_1	14.355
	K_T	0.6634
	R^2	0.9925
	Chi-sqr	0.373

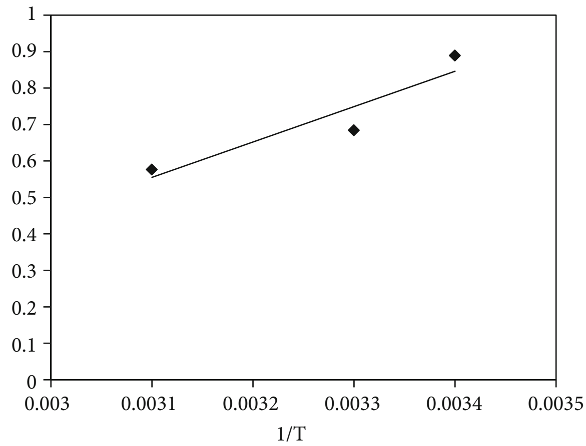

Figure 9: Thermodynamic plot of *Neolamarckia cadamba* for the adsorption of methylene blue.

Table 6: Thermodynamic parameters for the removal of methylene blue on *Neolamarckia cadamba* leaves.

Temperature (K)	K_c	ΔG° (kJ Mol^{-1} K^{-1})	ΔH° (kJ Mol^{-1} K^{-1})	ΔS° (kJ Mol^{-1})	R^2
293	7.7504	-4.9882	-18.5782	-0.0469	0.8704
303	4.8336	-3.9689			
313	3.7728	-3.4553			

Table 7: Comparative study of adsorption capacity ($q_{\max}$) of *Neolamarckia cadamba* with other adsorbents.

Adsorbent	$q_{\max}$ (mg/g)	References
Lathyrus sativus husk	98.33	[4]
Magnetic mesoporous silica (SBA-15-HESI-Fe_3O_4)	172.3	[16]
Activated carbon of lemon peels	38	[17]
Gnetum gnemon shell waste	35.58	[28]
Luffa acutangula carbon	10.32	[29]
Goethite	75.80	[30]
Salix babylonica	42.74	[31]
Salix alba L	35.46	[31]
H_3PO_4-treated eucalyptus leaves (PEUL)	194.34	[32]
Neolamarckia cadamba leaves	101.4	This study

log C_e is plotted as shown in Figure 8(b), and values are tabulated in Table 5.

The Temkin isotherm model is used to investigate the absorbent's adsorption potential on adsorbate. The nonlinear equation of Temkin is given as

$$q_e = \frac{RT}{b_T} \ln A_T C_e. \tag{9}$$

According to the data fitted, the adsorption of MB onto NC leaves was best fitted by the Langmuir isotherm model confirming the formation of a monolayer during the adsorption process. As Langmuir has a higher regression coefficient (R^2), this suggests the Langmuir isotherm is the best choice for fitting the data. The maximum adsorption capacity ($q_{\max}$) came out to be 101.4 mg g^{-1} which was higher than several other adsorbents (Table 5).

The fact that the Langmuir isotherm model fitted well for the adsorption of MB onto NC leaves attributes to the distribution of the active site on the adsorbent surface making it analogous [26].

3.6. Thermodynamic Study. In between the range of 293 and 313 Kelvin temperature, thermodynamic studies were conducted and the following equations were used to calculate the parameters such as enthalpy change (ΔH°), entropy change (ΔS°), and Gibbs free energy change (ΔG°):

$$\Delta G^\circ = -RT \ln K_c, \tag{10}$$

$\log K_c = \Delta S^\circ / 2.303R - \Delta H^\circ / 2.303RT$,where the equilibrium constant is denoted by the abbreviation (K_c), solid-phase concentration is denoted by C_s at equilibrium (mg/L), and C_e is the equilibrium concentration of the solution (mg/L). From the plot of log K_c vs. $1/T$, H° and ΔS° are computed as shown in Figure 9 and presented in Table 6.

The data reported in Table 6 show that ΔG° values are negative and decrease with increasing temperature. Also, the values of ΔH° and ΔS° are negative, which confirms the exothermic reaction and randomness at the solution interface during the adsorption of MB ions, as reported by Guiza [27].

3.7. Comparative, Disposal, and Feasibility of the Adsorbent. The adsorbent-feasibility check can be done by comparing monolayer adsorption capacity (NC) with the capacities of the other adsorbent for the removal of MB as reported in Table 7.

An acceptable disposal method might be biochar derived from dye-loaded adsorbents. Biochar prepared from dye-loaded adsorbents is useful for avoiding secondary pollution effects caused by MB-loaded adsorbents, for reducing depleted adsorbents, and for purifying dye. A suitable disposal method for contaminated adsorbents may be this method. In recent years, biochar technologies prepared from depleted adsorbents have been proposed and successfully used to remove dye from wastewater.

4. Conclusion

In this study, we have examined the sustainable use of waste biomass to treat industrial wastewater. According to the results, NC leaves are good adsorbents for removing MB and reducing TDS, conductivity, hardness, and COD in sewage belts in the Yamuna River like Kachar, Chachar, and Kareli in Allahabad, U.P., India. As a result of the treatment with NC leaves, the water quality of the sewage belts was purified. The maximum removal was obtained at pH 5 and 120-minute equilibrium time. The adsorbent followed a pseudo-second-order kinetic model with a regression coefficient of 0.999. The adsorbent was best fitted by Langmuir isotherm with a monolayer adsorption capacity of 101 mg/g at 50 ppm of MB concentration. The thermodynamic data revealed the reaction to be exothermic. An increase in temperature is directly proportionate with a decrease in spontaneity and decreased randomness at adsorbent-adsorbate interaction. As a result of the acquired results, it appears that biomass has a high capability to adsorb dye molecules from wastewater, which makes it a promising adsorbent for decolorization process.

Data Availability

The data is attached in the manuscript.

Conflicts of Interest

There is no conflict of interest.

Acknowledgments

I owe sincere thanks to the Department of Chemistry of SHUATS, Allahabad, India, for providing assistance in carrying out the work. The authors are thankful to the Deanship of Scientific Research (DSR), Majmaah University, Saudi Arabia, for supporting this work under Project Number R-2022-246.

References

[1] R. Isaac and S. Siddiqui, "Application of water quality index and multivariate statistical techniques for assessment of water quality around Yamuna river in Agra region, Uttar Pradesh, India," *Water Supply*, vol. 22, no. 3, pp. 3399–3418, 2022.

[2] B. Chakraborty, S. Roy, A. Bera et al., "Eco-restoration of river water quality during COVID-19 lockdown in the industrial belt of eastern India," *Environmental Science and Pollution Research*, vol. 28, no. 20, pp. 25514–25528, 2021.

[3] I. M. Alarifi, Y. O. Al-Ghamidi, R. Darwesh, M. O. Ansari, and M. K. Uddin, "Properties and application of MoS_2 nanopowder: characterization, Congo red dye adsorption, and optimization," *Journal of Materials Science and Technology*, vol. 13, pp. 1169–1180, 2021.

[4] I. Ghosh, S. Kar, T. Chattarjee, N. Bar, and S. K. Das, "Removal of methylene blue from aqueous solution using *Lathyrus sativus* husk: adsorption study, MPR and ANN modelling," *Process Safety and Environment Protection*, vol. 149, pp. 345–361, 2021.

[5] M. K. Uddin and A. Nasar, "Walnut shell powder as a low-cost adsorbent for methylene blue dye: isotherm, kinetics, thermodynamic, desorption and response surface methodology examinations," *Scientific Reports*, vol. 10, no. 1, p. 7983, 2020.

[6] M. K. Uddin and A. Nasar, "Decolorization of basic dyes solution by utilizing fruit seed powder," *KSCE Journal of Civil Engineering*, vol. 24, no. 2, pp. 345–355, 2020.

[7] R. A. K. Rao, F. Rehman, and M. Kashifuddin, "Removal of Cr(VI) from electroplating wastewater using fruit peel of Leechi (Litchi chinensis)," *Desalination and Water Treatment*, vol. 49, no. 1-3, pp. 136–146, 2012.

[8] A. Khatoon, M. K. Uddin, and R. A. K. Rao, "Adsorptive remediation of Pb(II) from aqueous media using *Schleichera oleosa* bark," *Environmental Technology and Innovation*, vol. 11, pp. 1–14, 2018.

[9] M. K. Uddin and P. Rahaman, "A study on the potential applications of rice husk derivatives as useful adsorptive material," in *Inorganic Pollutants in Wastewater: Methods of Analysis, Removal and Treatment*, M. A. Inamuddin and A. M. Asiri, Eds., Materials Research Forum LLC, 2017.

[10] R. A. K. Rao, S. Ikram, and M. K. Uddin, "Removal of Cd(II) from aqueous solution by exploring the biosorption characteristics of gaozaban (*Onosma bracteatum*)," *Journal of Environmental Chemical Engineering*, vol. 2, no. 2, pp. 1155–1164, 2014.

[11] R. A. K. Rao and M. Kashifuddin, "Adsorption properties of coriander seed powder (Coriandrum sativum): extraction and pre-concentration of Pb(II), cu(II) and Zn(II) ions from aqueous solution," *Adsorption Science and Technology*, vol. 30, no. 2, pp. 127–146, 2012.

[12] M. K. Uddin, N. N. Abd Malek, A. H. Jawad, and S. Sabar, "Pyrolysis of rubber seed pericarp biomass treated with

sulfuric acid for the adsorption of crystal violet and methylene green dyes: an optimized process," *International Journal of Phytoremediation*, pp. 1–10, 2022.

[13] S. H. Mosavi, R. Z. Dorabei, and M. Bereyhi, "Rapid and effective ultrasonic-assisted adsorptive removal of Congo red onto MOF-5 modified by $CuCl_2$ in ambient conditions: adsorption isotherms and kinetics studies," *ChemistrySelect*, vol. 6, no. 18, pp. 4432–4439, 2021.

[14] M. Bereyhi, R. Z. Dorabei, and S. H. Mosavi, "Microwave-assisted synthesis of CuCl-MIL-47 and application to adsorptive denitrogenation of model fuel: response surface methodology," *ChemistrySelect*, vol. 5, no. 46, pp. 14583–14591, 2020.

[15] R. Z. Dorabei and S. Nazerdeylami, "Simultaneous adsorption of Hg^{2+}, Cd^{2+} and Cu^{2+} ions from aqueous solution with mesoporous silica/DZ and conditions optimise with experimental design: kinetic and isothermal studies," *Micro & Nano Letters*, vol. 14, no. 8, pp. 823–827, 2019.

[16] S. Nourozi and Z. R. Dorabei, "Highly efficient ultrasonic-assisted removal of methylene blue from aqueous media by magnetic mesoporous silica: experimental design methodology, kinetic and equilibrium studies," *Desalination and Water Treatment*, vol. 85, pp. 184–196, 2017.

[17] D. M. Ramutshatsha, A. Mavhungu, M. L. Moropeng, and R. Mbaya, "Activated carbon derived from waste orange and lemon peels for the adsorption of methyl orange and methylene blue dyes from wastewater," *Heliyon*, vol. 8, no. 8, article e09930, 2022.

[18] M. O. Omorogie, J. O. Babalola, M. O. Ismaeel et al., "Activated carbon from *Nauclea diderrichii* agricultural waste -a promising adsorbent for ibuprofen, methylene blue and CO_2," *Advanced Powder Technology*, vol. 32, no. 3, pp. 866–874, 2021.

[19] X. Peng, L. L. Ye, C. H. Wang, H. Zhou, and B. Sun, "Temperature- and duration-dependent rice straw-derived biochar: characteristics and its effects on soil properties of an Ultisol in southern China," *Soil and Tillage Research*, vol. 112, no. 2, pp. 159–166, 2011.

[20] Y. Chenglong and W. Huaijian, "agricultural waste derived catalysts for low temperature SCR process: optimization of preparation process, catalytic activity and characterization," *Aerosol and Air Quality Research*, vol. 20, no. 4, pp. 862–876, 2020.

[21] G. Karaçetin, S. Sivrikaya, and M. Imamoğlu, "Adsorption of methylene blue from aqueous solutions by activated carbon prepared from hazelnut husk using zinc chloride," *Journal of Analytical and Applied Pyrolysis*, vol. 110, pp. 270–276, 2014.

[22] F. Bouaziz, M. Koubaa, F. Kallel et al., "Efficiency of almond gum as a low-cost adsorbent for methylene blue dye removal from aqueous solutions," *Industrial Crops and Products*, vol. 74, pp. 903–911, 2015.

[23] V. K. Gupta, A. Rastogi, and A. Nayak, "Adsorption studies on the removal of hexavalent chromium from aqueous solution using a low cost fertilizer industry waste material," *Journal of Colloid and Interface Science*, vol. 342, no. 1, pp. 135–141, 2010.

[24] K. S. George, K. B. Revathi, N. Deepa, C. P. Sheregar, T. S. Ashwini, and S. Das, "A study on the potential of Moringa leaf and bark extract in bioremediation of heavy metals from water collected from various lakes in Bangalore," *Procedia Environmental Sciences*, vol. 35, pp. 869–880, 2016.

[25] G. O. El-sayed, "Removal of methylene blue and crystal violet from aqueous solutions by palm kernel fiber," *Desalination*, vol. 272, no. 1-3, pp. 225–232, 2011.

[26] S. N. do Carmo Ramos, A. L. P. Xavier, F. S. Teodoro, L. F. Gil, and L. V. A. Gurgel, "Removal of cobalt(II), copper(II), and nickel(II) ions from aqueous solutions using phthalate-functionalized sugarcane bagasse: mono- and multicomponent adsorption in batch mode," *Industrial Crops and Products*, vol. 79, pp. 116–130, 2016.

[27] S. Guiza, "Biosorption of heavy metal from aqueous solution using cellulosic waste orange peel," *Ecological Engineering*, vol. 99, pp. 134–140, 2017.

[28] R. Lelifajri, S. Supriatno, and A. S. M. Indarum, "Study on methylene blue dye adsorption in aqueous solution by heat-treated Gnetum gnemon shell waste particles as low-cost adsorbent," *AIP Conference Proceedings*, vol. 2243, no. 1, article 020012, 2020.

[29] S. H. Siddiqui, "The removal of Cu^{2+}, Ni^{2+} and methylene blue (MB) from aqueous solution using luffa Actangula carbon: kinetics, thermodynamic and isotherm and response methodology," *Groundwater for Sustainable Development*, vol. 6, pp. 141–149, 2018.

[30] D. Kharisma, Z. Abidin, and C. Kusmana, "Adsorption of methylene blue onto a low-cost and environmental friendly goethite," *IOP Conference Series: Earth and Environmental Science*, vol. 399, no. 1, article 012013, 2019.

[31] B. T. Gemici, H. U. Ozel, and H. B. Ozel, "Removal of methylene blue onto forest wastes: adsorption isotherms, kinetics and thermodynamic analysis," *Environmental Technology and Innovation*, vol. 22, article 101501, 2021.

[32] K. Ghosh, N. Bar, A. B. Biswas, and S. K. Das, "Removal of methylene blue (aq) using untreated and acid-treated eucalyptus leaves and GA-ANN modelling," *Canadian Journal of Chemical Engineering*, vol. 97, no. 11, pp. 2883–2898, 2019.